Macromolecules

ARTICLE

pubs.acs.org/Macromolecules

Highly Ordered Nanoporous Thin Films from Photocleavable Block Copolymers

Hui Zhao,[†] Weiyin Gu,[‡] Elizabeth Sterner,[‡] Thomas P. Russell,[‡] E. Bryan Coughlin,[‡,*] and Patrick Theato[†,§,∥,*]

[†]Institute of Organic Chemistry, University of Mainz, Duesbergweg 10-14, D-55099 Mainz, Germany

[‡]Department of Polymer Science & Engineering, University of Massachusetts, 120 Governors Drive, Amherst Massachusetts 01003-4530, United States

[§]World Class University (WCU) program of Chemical Convergence for Energy & Environment (C_2E_2), School of Chemical and Biological Engineering, College of Engineering, Seoul National University (SNU), Seoul, Korea

[∥]Institute for Technical and Macromolecular Chemistry, University of Hamburg, Bundesstr. 45, 20146 Hamburg, Germany

Supporting Information

ABSTRACT: Poly(styrene-*block*-ethylene oxide) with an *o*-nitrobenzyl ester photocleavable junction (PS-*hν*-PEO) was synthesized by a combined RAFT polymerization and "click chemistry" approach and represents the first report utilizing this method for the synthesis of photocleavable block copolymers. After solvent annealing, highly ordered thin films were prepared from PS-*hν*-PEO. Following a very mild UV exposure and successive washing with water, PS-*hν*-PEO thin films were transformed into highly ordered nanoporous thin PS films with pore diameters of 15−20 nm and long range ordering (over 2 μm × 2 μm). Afterwards the pores were filled with PDMS by spin-coating in combination with capillary forces. After treatment with oxygen plasma to remove the PS templates, highly ordered arrays of silica nanodots were obtained. This represents the first template application example from highly ordered nanoporous thin films derived from block copolymers featuring a photocleavable junction.

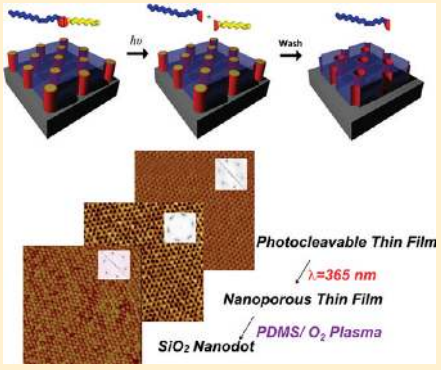

INTRODUCTION

Highly ordered nanoporous thin films through self-assembly of block copolymers (BCPs) have received continuous attention since they are a promising platform for the "bottom-up" fabrication of nanostructured materials and devices.[1] However, several challenges have to be addressed before nanoporous thin films can be used for fabrication of advanced templates and devices. One of the most severe challenges is the selective removal of one domain under mild and technologically compatible conditions. Until now, diverse methods have been developed for the selective removal of one domain, such as chemical etching,[2] ozonolysis,[3] and UV degradation.[4] However, most of these methods require relatively harsh conditions, or are limited to degradable polymers, such as poly(methyl methacrylate), poly(1,4-isoprene), and poly(lactic acid). To overcome these drawbacks, the approach of introducing an efficiently cleavable linker between the two blocks has been developed.[5,6] In particular, the strategy based on photocleavable junctions is a very promising platform for the synthesis of nanoporous materials (Chart 1).[6]

Among the many photocleavable groups available, *o*-nitrobenzyl (ONB) alcohol derivatives have gained tremendous attention in the area of synthetic organic chemistry.[7] Moon and co-workers were the first to demonstrate the possibility of obtaining photocleavable BCP thin films based on ONB.[6a] They synthesized a photocleavable polystyrene-*block*-poly(ethylene oxide) diblock copolymer by ATRP using an ONB-functional PEO macroinitiator. Recently, Fustin and co-workers developed a one pot ATRP−CuAAC "click" method to synthesize photocleavable BCPs.[6b] The pioneering work of Moon and Fustin shows that the introduction of an ONB junction to BCPs is a promising method to prepare nanoporous thin films.

RAFT polymerization is generally considered to have certain potential benefits over ATRP in the controlled polymerization of functional monomers.[8] However, the synthesis of RAFT chain transfer agents (CTAs) is difficult, in particular for macromolecular CTAs, which often requires multiple steps of end-group modification. Developing CTAs suitable for the synthesis of photocleavable BCPs based on ONB remains a challenge that has not yet been addressed, in particular by combining RAFT polymerization and "click" chemistry[9] for this purpose. A combined "RAFT-click" method has two advantages: (a) it can avoid the synthesis of a macro-CTA, which is difficult to purify since they often need multiple steps of macromolecular reactions (Scheme 1, route A), and (b) it represents a platform method capable to provide easy access to series of different photocleavable BCPs.

In this work, we successfully developed a "RAFT-click" method to synthesize photocleavable BCPs (Scheme 1, route B) and compared it to the sequential route using a macro-CTA

Received: June 22, 2011
Revised: July 20, 2011
Published: July 28, 2011

Chart 1. Schematic Representation of the Self-Assembly of Photocleavable Block Copolymers and the Subsequent Removal of One Domain after UV Irradiation

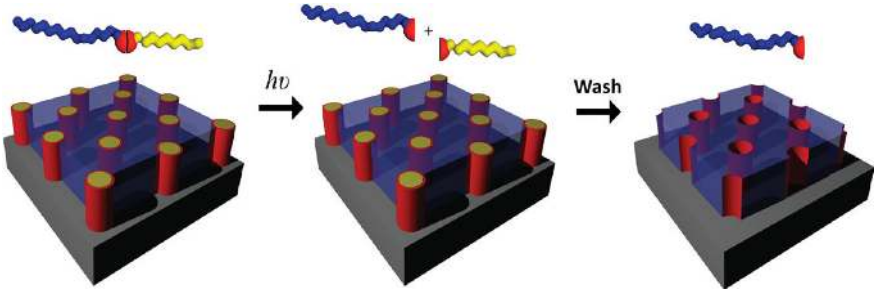

Scheme 1. Two RAFT Polymerization Routes for the Synthesis of Photocleavable PS-*hν*-PEO

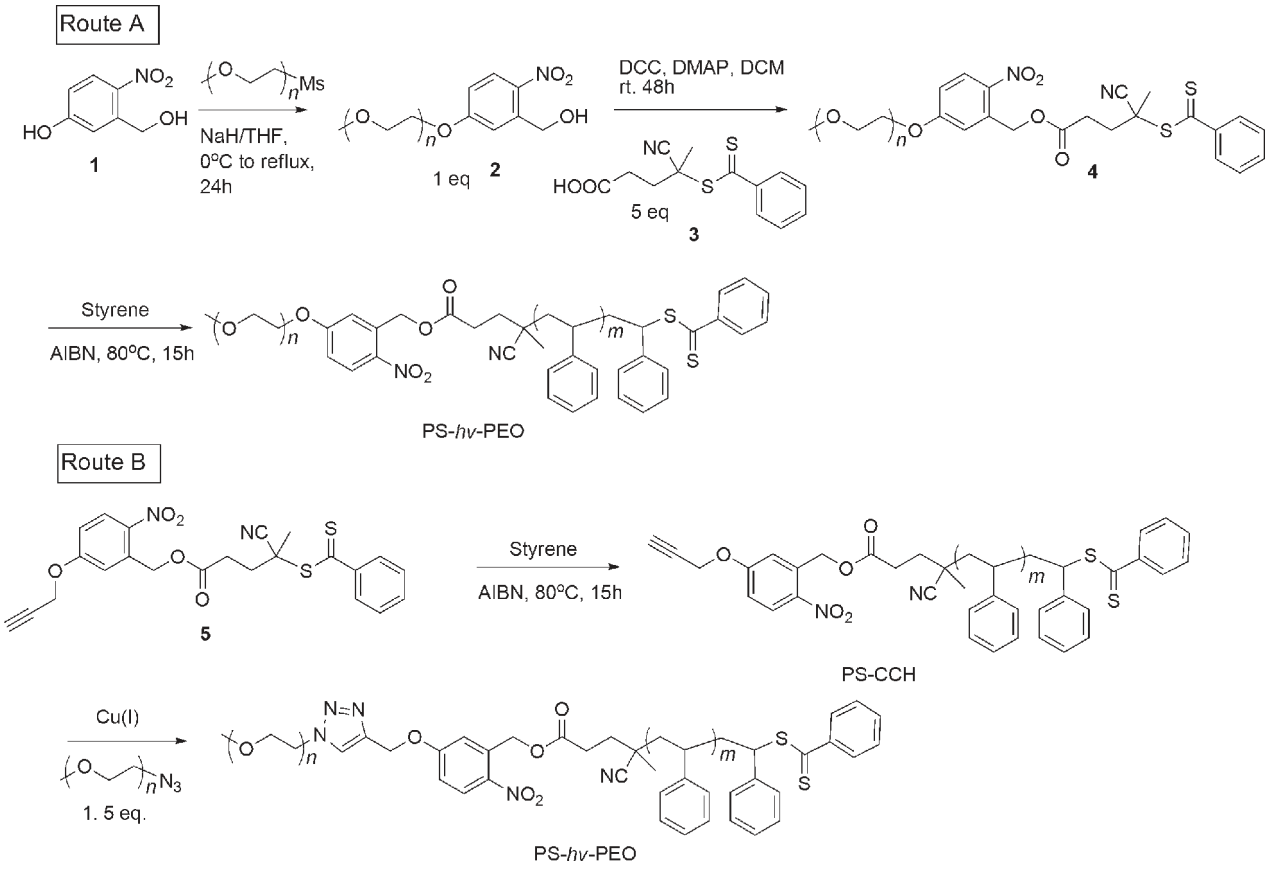

approach. The resulting photocleavable BCPs were then used to prepare highly ordered thin films. Following exposure to UV light and washing with water these materials are expected to lead to highly ordered nanoporous thin films (see Chart 1). As a demonstration of the utility of the nanoporous array, a replication technique resulting in silica nanodots was investigated using a simple spin coating procedure with polydimethylsiloxane and treatment with oxygen plasma.

RESULTS AND DISCUSSION

Polymer Synthesis and Photolysis in Solution. To demonstrate the versatility of the "RAFT-click" approach yielding photocleavble BCPs, two different routes involving RAFT polymerization to produce PS-*hν*-PEO have been investigated. We have employed the nomenclature of "*hν*" in place of the common italic "*b*" to denote a BCP with a photocleavable junction point between the two blocks. In the first route, we used traditional RAFT polymerization utilizing a macro-CTA (Scheme 1, route A) and in the second route we used a combined RAFT polymerization-"click chemistry" approach (Scheme 1, route B). For route A, a macromolecular chain transfer agent (**4**) was synthesized in two steps from monomethyl ether poly(ethylene oxide), and 4-cyano-4-(phenylcarbonothioylthio)-pentanoic acid (**3**) and 3-hydroxymethyl-4-nitrophenol (**1**). The overall yield of **4** was very low due to multiple reactions on macromolecular end-groups and coproduction of a disulfide dimer (**9**) (see Supporting Information, Scheme S1). A hypothesis for this dimerization mechanism yielding polymeric disulfides was proposed

Scheme 2. Synthesis of CTA 5

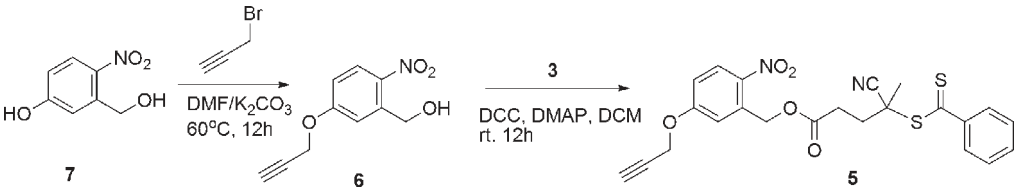

Table 1. Synthesis of the Alkyne End-Group Functionalized Polystyrenes (PS−C≡CH) and Block Copolymers (PEO-*hν*-PS) Bearing a Photocleavable ONB Junction[a]

PS alkyne	$[St]_0/[CTA]$	M_n[b] (g/mol)	Đ[b]	PS-*hν*-PEO	M_n[b] (g/mol)	Đ[b]
PS−C≡CH(P**1**)	240	5200	1.17	P**1**-*hν*-PEO	15 000	1.30
PS−C≡CH(P**2**)	480	12 000	1.12	P**2**-*hν*-PEO	22 000	1.22
PS−C≡CH(P**3**)	600	14 400	1.13	P**3**-*hν*-PEO	24 000	1.23
PS−C≡CH(P**4**)	720	15 700	1.12	P**4**-*hν*-PEO	27 000	1.22
PS−C≡CH(P**5**)	1080	23 700	1.19	P**5**-*hν*-PEO	33 000	1.30
PS−C≡CH(P**6**)	1200	26 800	1.20	P**6**-*hν*-PEO	37 000	1.30

[a] RAFT polymerization was carried out at 80 °C with a ratio [AIBN]:[CTA] of 1:8, conversion of styrene was around 20%; "click" coupling between 5000 g/mol (M_n = 9500 g/mol for GPC in chloroform) PEO−N_3 and PS (PS−C≡CH) was carried out at room temperature in the presence of CuBr/PMDETA (*N*,*N*,*N*′,*N*′,*N*″-pentamethyldiethylenetriamine) (molar ratio: 1/1). [b] GPC in chloroform using linear PS standards.

(Scheme S1, Supporting Information) and verified by an obvious GPC change after adding DL-dithiothreitol (DTT) due to the reductive cleavage of the proposed disulfide bond (Scheme S2 and Figure S1, Supporting Information). It is very difficult to remove the polymeric disulfide **9** from the desired CTA **4** due to the subtle difference in molecular weight (29K vs 16K) and their very similar solubility properties. Accordingly, all attempts to use the mixture for a RAFT polymerization of styrene resulted in poor control over the polymerization (PDI >1.5).

Compared with route A, the advantages of route B are the straightforward synthesis of the CTA in high yield (Scheme 2), the RAFT polymerization using CTA (**5**) is well controlled (Table 1 and Figure S3, Supporting Information), and the "RAFT-click" method represents a versatile platform for the production of a broad range of photocleavable BCPs by replacing PEO−N_3 with other polymers featuring an azide end-group as well as replacing styrene with other functional monomers for RAFT polymerization. The RAFT polymerization of styrene and "click" coupling with PEO−N_3 were successful and the resulting polymers were characterized by ^{1}H NMR and GPC. Polystyrene P**4** (Table 1, PS, $M_{n,GPC}$ = 15 700 g/mol). The block copolymer P**4**-*hν*-PEO will be discussed in the following as a typical representative for all synthesized block copolymers.

^{1}H NMR spectra of the photocleavable RAFT agent **5**, PS (P**4**), and P**4**-*hν*-PEO are shown in Figure 1. All protons of compound **5** could be assigned (see Figure 1A). Polystyrene with ONB end-group was prepared by RAFT polymerization using CTA **5**. The ^{1}H NMR spectrum of P**4** (see Figure 1B) revealed besides the resonances for PS at δ = 1.17−2.0 ppm (main chain) and at δ = 6.30−7.50 ppm (side chain phenyl group) that the alkyne end-group (Figure 1B, resonance **11**) remained intact after RAFT polymerization. After the "click" reaction with PEO−N_3, the resonance **11** disappeared in the ^{1}H NMR (see Figure 1C). Further, the chemical shift of the methylene protons (peak **12** in Figure 1B) close to the triple bond shifted from 4.76 to

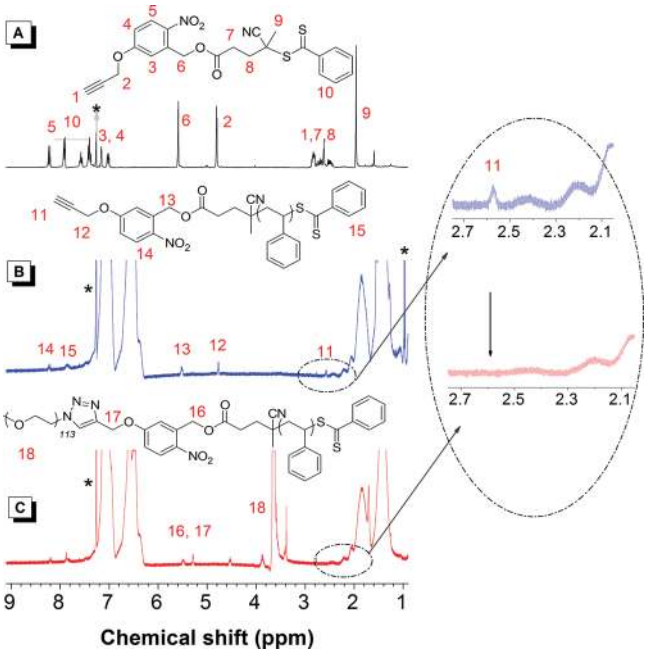

Figure 1. ^{1}H NMR (all in $CDCl_3$) for (A) CTA **5**, (B) alkyne end-group functionalized polystyrene (P**4**) prepared by RAFT polymerization, and (C) PS-*hν*-PEO (P**4**-*hν*-PEO) by "click" chemistry with PEO−N_3.

5.29 ppm (peak **17** in Figure 1C) due to the presence of the electron-withdrawing 1,2,3-triazole ring. According to ^{1}H NMR, the yield of "click" coupling between PEO−N_3 and alkyne end functionalized PS was nearly quantitative.

As summarized in Table 1, PS with different molecular weights (5 kDa to 27 kDa, Đ below 1.20) were prepared by RAFT polymerization utilizing CTA **5**. The polymerizations were carried out at 80 °C in both the bulk and using dioxane as a solvent with a [AIBN]:[CTA] ratio of 1:8. The highest

dx.doi.org/10.1021/ma201416b |*Macromolecules* 2011, 44, 6433–6440

conversion in the bulk was nearly the same as that in dioxane (about 20%). Given the fact that nitrobenzene can act as an inhibitor for radical polymerization, ONB might affect RAFT polymerization. To check the effect of ONB on the polymerization, a reaction was performed in the presence of compound **3** using the same polymerization conditions as with CTA **5**. The conversion in the presence of **3** is also approximately 20%. Thus, we concluded that ONB did not have a negative effect the RAFT polymerization, which is in agreement with the ^{1}H NMR data shown in Figure 1B.

Next, "click" coupling between PEO−N_3 and P**4** (PS−C≡CH) was performed at room temperature in the presence of CuBr/PMDETA (*N*,*N*,*N*′,*N*′,*N*″-pentamethyldiethylenetriamine) (molar ratio: 1/1) as catalyst. As amines tend to trigger aminolysis of the dithioester end-group of RAFT polymers resulting often in disulfide dimerization, polymers obtained by RAFT polymerization are often treated with AIBN to replace the dithioester end-group to avoid this side reaction.[9g] However, this adds one more step to the synthesis. To keep the synthesis route as short as possible, we omitted the step of AIBN radical substitution of the dithioester. Given CuBr/PMEDTA as the catalyst, we tried to reduce the amount of catalyst in the "click" coupling to prevent the use of any excess of PMDETA to eliminate side reactions. When the ratio between CuBr/PDEDTA and PS−C≡CH was 0.3:1(or lower), the "click" coupling worked very well (Table 1, Figure 2). The Đ of the resulting PS-*hν*-PEO diblock copolymers were between 1.22 to 1.30 with almost no indication of dimerization. Even though a small tailing toward higher molecular weights was still observed in the GPC (see Figure 2), it did not have an effect on the organization behavior of the diblock copolymers within thin films, *vide infra.*

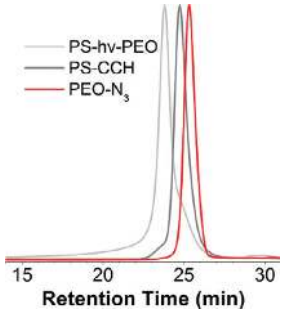

Figure 2. GPC trace of P**4**-*hν*-PEO ($M_{n,GPC}$ =27000, PDI = 1.22), PS−CCH (P**4**, $M_{n,GPC}$ = 15700, Đ= 1.12), and PEO−N_3 ($M_{n,GPC}$ = 9500, Đ=1.04) in chloroform using linear PS standards.

P**4**-*hν*-PEO was selected as an example to demonstrate the photolysis of the prepared photocleavable block copolymers in solution. Photolysis of P**4**-*hν*-PEO in dioxane was performed in a NMR tube under a common UV lamp (λ = 365 nm, 1.3 mW/cm^2). After 12 h, the cleaved polystyrene was collected by precipitating into MeOH. GPC analysis showed that P**4**-*hν*-PEO was cleaved completely under UV exposure resulting in PS (Figure 3, left). However, the PS obtained from photolysis of P**4**-*hν*-PEO was white (P**4** and P**4**-*hν*-PEO were pink), indicating that the CTA end-group might also have cleaved under UV exposure (Figure 3, right). GPC with refractive index (RI) and UV−vis (UV) (wavelength =512 nm, at dithio ester absorbance peak) detection were used in combination to detect the P**4**-*hν*-PEO and P**4** to prove this hypothesis (Figure 4). If the CTA was intact after UV exposure, the GPC−RI and GPC−UV should result in overlapping GPC traces. As can be seen from Figure 4, the PS collected from P**4**-*hν*-PEO after UV irradiation was nearly the same as P**4** in GPC−RI (Figure 4A). However, the UV−vis GPC trace measured after UV exposure had no signal, showing clearly that the CTA group was also cleaved during UV exposure. These results indicate that UV exposure is also a simple, nonchemical method for removing CTA groups from RAFT polymers, which is in agreement with the literature.[14]

Highly Ordered Nanoporous Thin Films and Application as Nanodot Template. PS-*b*-PEO BCPs have attracted considerable attention for the generation of highly ordered microphase separated thin films of nanocylinders oriented perpendicular to a substrate.[1] However, the PEO block is not easily removed by simple etching processes, limiting potential applications.[10] Russell and co-workers introduced PS-*b*-PMMA-*b*-PEO triblock system, in which PMMA could be degraded by short-wavelength UV exposure.[4b] Venkataraman and co-workers reported a PS-*b*-PEO system with an acid-sensitive trityl ether linkage, which can be cleaved by acid treatment.[5d] All these methods can selectively remove the PEO block and result in highly ordered nanoporous thin films, but they require harsh cleavage conditions. As demonstrated above, photolysis of PS-*hν*-PEO is successful under mild UV irradiation conditions. Accordingly, PS-*b*-PEO featuring an ONB cleavable junction seems a strong candidate for highly ordered nanoporous thin films. So far, only one example of thin films prepared from PS-*b*-PEO with an ONB junction has been

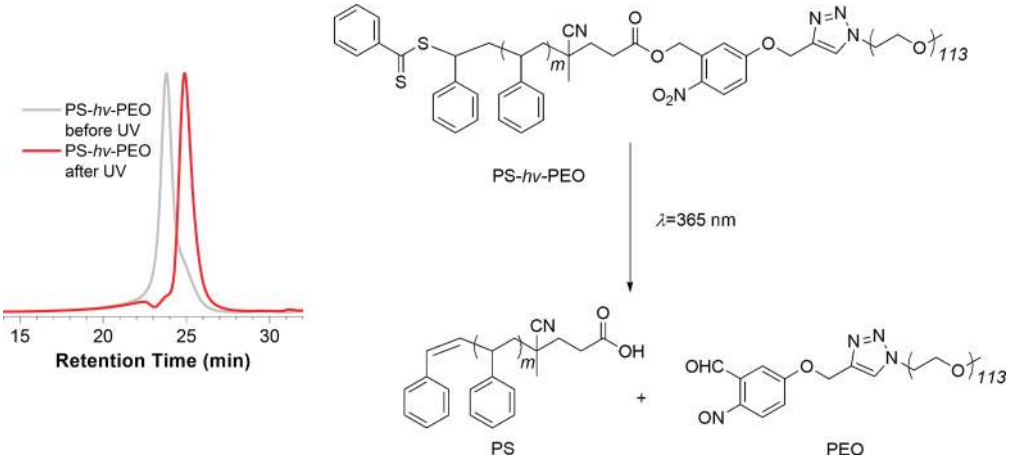

Figure 3. GPC trace in chloroform of PS-*hν*-PEO (P**4**-*hν*-PEO) before and after UV exposure using linear PS standard (left). Photolysis of PS-*hν*-PEO in solution (right).

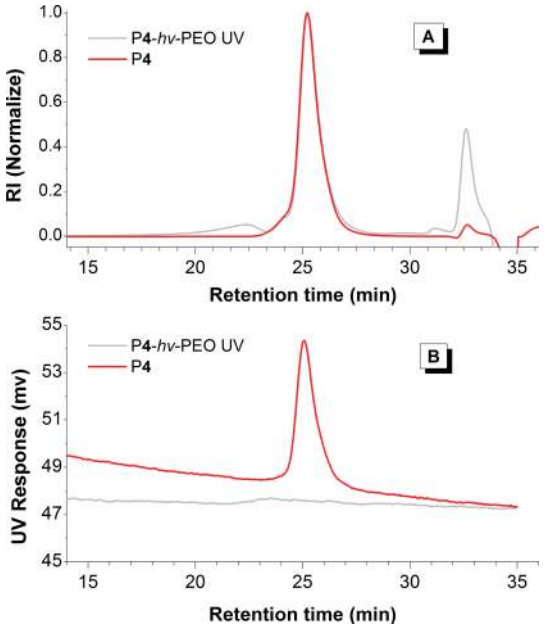

Figure 4. GPC−RI (A) and GPC−UV (wavelength = 512 nm, at dithio ester absorbance peak) and (B) traces of P**4** and P**4**-*hν*-PEO after UV exposure using linear PS standards.

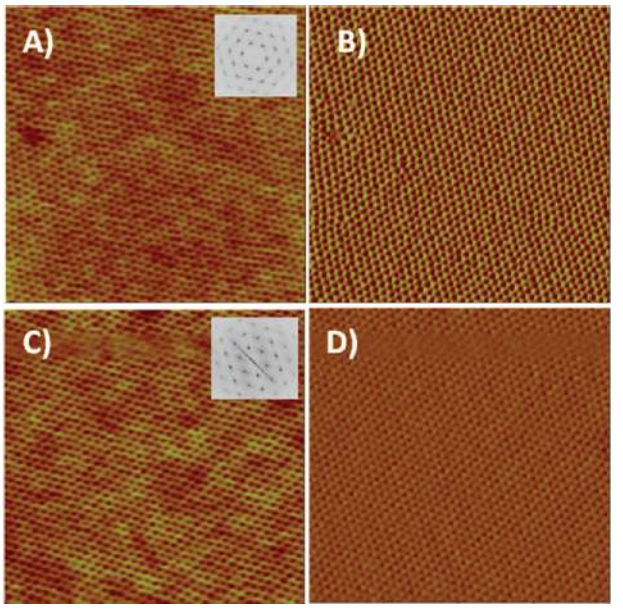

Figure 5. AFM height (A, C) and phase (B, D) images for PS-*hν*-PEO thin films (film thickness ∼30 nm) after annealing for 2.5 h in H_2O/THF atmosphere. Key: (A and B) P**5**-hv-PEO (24K−5K); (C and D) P**6**-*hν*-PEO (26.8K−5K). Scale: 1 μm × 1 μm. The insets in A and C show the corresponding 2D Fourier transform.

reported.[6a] However, the morphology of the thin films was not highly ordered, limiting its potential application. We therefore tried to find the best condition of solvent annealing to get highly ordered morphology in the thin film, which will lead to highly ordered templates after UV cleavage of the ONB junction.

PS-*hν*-PEO was spin-coated from toluene solution onto silicon wafers and a highly ordered morphology for these PS-*hν*-PEO thin films was obtained after annealing for 2.5 h at 20 °C

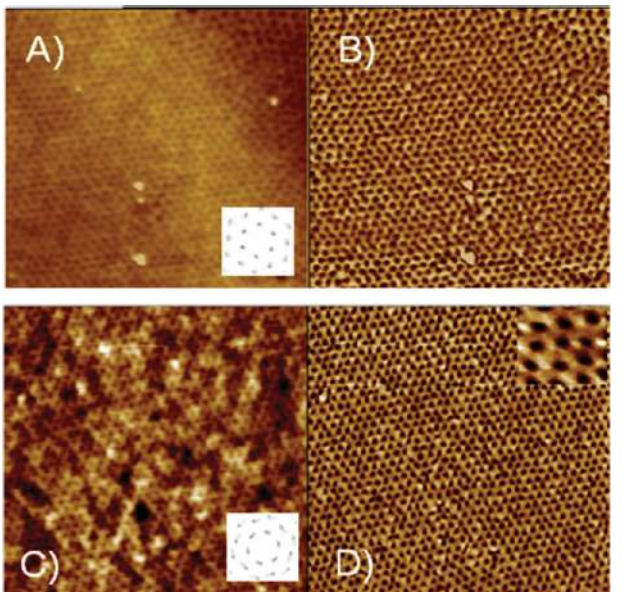

Figure 6. AFM height (A, C) and phase (B, D) images for PS-*hν*-PEO thin film (film thickness ∼30 nm) after UV exposure and washing with water. Key: (A and C) P**5**-*hν*-PEO (5K−24K); (B and D) P**6**-*hν*-PEO (5K−26.8K). The insets in parts A and C show the corresponding Fourier transform. Inset in D shows a magnified image at 100 nm × 100 nm. A−D scale: 1 μm × 1 μm.

in a H_2O/THF atmosphere. In particular, highly ordered hexagonally packed cylinders oriented perpendicular to the substrate were obtained for the block copolymers P**5**-*hν*-PEO and P**6**-*hν*-PEO (see Figure 5). The Fourier transforms of the AFM images are shown in the insets of Figure 5, parts A and C. Six-point patterns, with multiple higher-order reflections are clearly seen, which is characteristic of long-range lateral ordering.[11] This highly ordered morphology of PS-*hν*-PEO is a prerequisite for highly ordered nanoporous thin films.

The next step was selective removal of the PEO block from the PS-*hν*-PEO thin film using a simple two-step procedure. First, UV exposure (365 nm for 12 h) causes photocleavage. Second, the PEO phase is removed by washing the films with water. This mild procedure maintains the highly ordered morphology. As can be seen from AFM images in Figure 6, highly ordered nanoporous thin films with six point FT patterns were obtained after UV exposure and a successive water washing step. The pores in the film were 15−20 nm in diameter, similar to the diameter of the original PEO cylinders, and had very narrow domain size distributions. TEM images also showed highly ordered nanoporous morphology in the resulting PS thin film (see Figure 7). Noteworthy, the contrast between bright and dark domains was enhanced noticeably after UV exposure and washing with water, which indicates the enhanced electron contrast due to the removal of the PEO domain. The highly ordered array morphology was of long-range order (over 2 μm × 2 μm) as seen from TEM (see Supporting Information, Figure S6).

To demonstrate that the nanoporous structures were not the result of reconstruction of the thin film by drawing PEO to the surface of the film[11] but are instead a result of the PEO removal, high-resolution X-ray photoelectron spectroscopy (XPS) was performed. First, XPS measurements were performed on PEO, PS-*hν*-PEO and PS-*hν*-PEO after UV treatment at the bottom surface of the thin films at 75°. There were at least eight kinds of

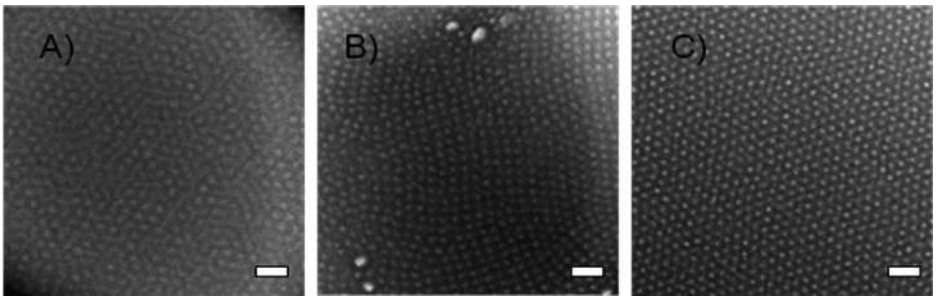

Figure 7. TEM images for PS-*hν*-PEO thin film before (A, P**5**-*hν*-PEO) and after UV exposure and water wash (B, P**5**-*hν*-PEO; C, P**6**-*hν*-PEO). Scale bar: 100 nm.

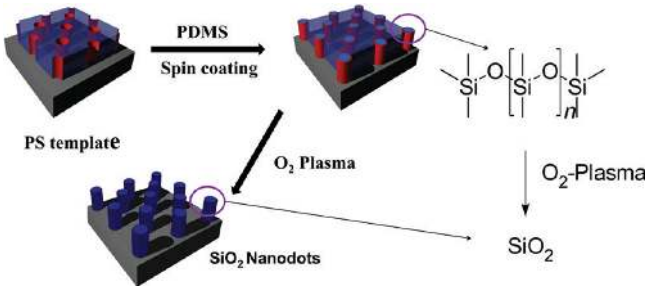

Figure 8. Schematic illustration for preparation of silica nanodots from a nanoporous PS template. Filling the pores with PDMS by spin-coating and subsequent conversion into silica nanodots by oxygen plasma treatment.

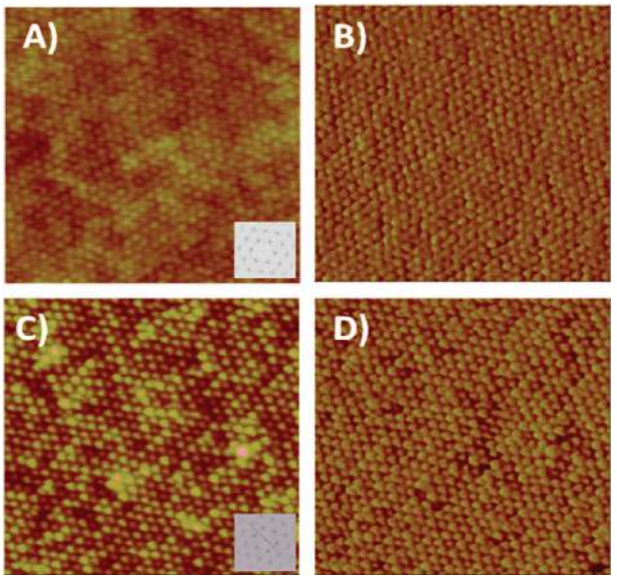

Figure 9. AFM height (A, C) and phase (B, D) images of silica nanodots obtained from PDMS by oxygen plasma treatment. The insets in A and C show the corresponding Fourier transform. Scale: 1 μm × 1 μm.

carbon related bonds in PS-*hν*-PEO: for the PS block, C−C, C−H bond in backbone and C−C, C−H bond in phenyl side group; for the PEO block, C−C bond and C−O, C−C, C−H bonds in backbone. A shoulder was observed at 286−284 eV (C−O bond) for PS-*hν*-PEO before UV irradiation, which vanished almost completely after UV irradiation (see Supporting Information, Figure S4). Next, the nanoporous thin films (PS-*hν*-PEO films post-UV treatment) were analyzed at the top surface by XPS at 15° (see Supporting Information, Figure S5). The spectra obtained from the surface were the same as the spectra from the bottom surface, allowing us to conclude that the holes resulted from PEO removal and extend from surface to bulk in the film.

The highly ordered morphology in the nanoporous thin film makes it a good candidate to be used as a nanoscale template. As a proof of concept, silica nanodot arrays were produced from the PS template. As illustrated in Figure 8, the silica nanodots were prepared using a PS template in two steps: a) spin-coating PDMS from heptane solution on the nanoporous thin film; b) removing the PS template and oxidizing PDMS by treatment with an oxygen plasma (1 h, 30 W, 0.2 bar O_2). The resulting SiO_2 nanodots were then imaged by AFM (Figure 9). It should be noted that the morphology of the resulting nanodots persisted with the long-range lateral order transferred from the template, as evidenced by the Fourier transform patterns, demonstrating these PS-*hν*-PEO block copolymers are good candidates for utilization as nano-templates with long-range order.

■ CONCLUSIONS

The development of a versatile method to produce photo-cleavable block copolymers via "RAFT-click" combination is a platform methodology that allows the fabrication of highly ordered arrays of nanopores via the self-assembly of photocleavable block copolymer thin films. Under mild UV treatment and subsequent washing with water, nearly perfect hexagonal arrays of ∼15 nm diameter holes were obtained. Highly ordered silica nanodots were then prepared utilizing these nanoporous thin films, which showed that the high degree of order of the nanoporous films can be transferred from the template nanodot array.

■ EXPERIMENTAL SECTION

Materials and Characterization. Styrene was filtered through basic aluminum oxide before polymerization, and 2,2′-azobis-(isobutyronitrile) (AIBN) was recrystallized from methanol. Triethylamine and dichloromathane (DCM) were distilled from calcium hydride. Tetrahydrofuran (THF) was distilled from sodium benzophenone ketyl. PEO monomethyl ether (5000 g/mol) was purchased from Sigma-Aldrich. All other reagents were purchased from commercial sources and used as received unless otherwise noted. The ^{1}H NMR was measured on a Bruker 300 MHz NMR spectrometer using tetramethylsilane (TMS; $\delta = 0$ ppm) as internal standard. The average molecular weights (M_w and M_n) and dispersities ($Đ$) of the polymers were estimated by a Waters Associates GPC system in chloroform. A set of monodisperse polystyrene standards covering molecular weight range of 10^3−10^7 g/mol was

used for the molecular weight calibration mode. Films for transmission electron microscopy (TEM) were prepared on silicon substrates having a thick layer of silicon oxide. These films were floated off the surface with a 5 wt % HF solution, transferred to a water bath, and then picked up on a Cu grid. A JEOL 100CX electron microscope operating at 100 kV was used to examine the morphology. Scanning force microscopy was performed on a Digital Instruments Dimension 3100, operating in tapping mode. The XPS analysis was carried out in a Physical Electronics apparatus with a nonmonochromatic Mg Kα radiation source at 15° and 75° take off angle. The sensitivity factors specified for the spectrometer were used for quantitative analysis. The pressure in the analysis chamber was less than 10^{-5} Pa. The spectrum collection time was kept under 10 min to minimize X-ray damage.

CTA Synthesis. 3-Hydroxymethyl-4-nitrophenol (**1**), PEO−ONB−OH (**2**), compound **3**, PEO−Ms, PEO−N_3, and compound **6** were prepared according to previously published methods.[6,12,13]

*Macromolecular CTA (**4**).* Into a 250 mL round-bottom flask were placed 2 g (0.4 mmol) of PEO−ONB−OH (**2**), 1.1 g (4 mmol) of compound **3**, 400 mg (2 mmol) of 1,3-dicyclohexylcarbodiimde (DCC), 50 mg (0.4 mmol) of 4-(dimethylamino)pyridine (DMAP), and 150 mL of DCM. The resulting solution was stirred at room temperature for 48 h. After filtration, the solution was extracted three times by DCM/water followed by removal of DCM in vacuum. The residue was diluted with DCM and precipitated from diethyl ether. A light pink powder (1 g, yield∼50%) was obtained after filtration and dried one night in vacuum at 30 °C. ^{1}H NMR (300 MHz, $CDCl_3$), δ (TMS, ppm): 8.20 (d, ArH), 7.90 (d, ArH), 7.60−7.31 (m, ArH), 7.05 (s, ArH), 6.95 (d, ArH), 5.5 (s, −CH_2O), 4.20−3.38 (CH_2O in PEO), 3.35 (s, OCH_3), 2.15 (s, C(CN)CH_3).

*ONB-CTA (**5**).* Into a 50 mL round-bottom flask were placed 830 mg (4 mmol) of compound **6**, 1.2 g (4.4 mmol) of compound **3**, 800 mg (4 mmol) of 1,3-dicyclohexylcarbodiimde (DCC), 50 mg (0.4 mmol) of 4-(dimethylamino)pyridine (DMAP) and 20 mL DCM. The resulting solution was stirred at room temperature for 16 h. DCM was removed under reduced pressure and the residue was collected and purified on a silica gel column using chloroform as eluent. A pink highly viscous compound was obtained in 83% yield (1.5 g). ^{1}H NMR (300 MHz, $CDCl_3$), δ (TMS, ppm): 8.24 (d, 1H, ONB), 7.92 (d, 2H, SS−ArH), 7.60 (t, 1H, SS−ArH), 7.43 (t, 2H, SS−ArH), 7.15 (s, 1H, ONB), 7.03 (d, 1H, ONB), 5.58 (s, 2H, ONB−CH_2−O), 4.80 (s, 2H, HCC−CH_2−ONB), 2.86−2.43 (m, 5H, OOC−CH_2−CH_2, HCC−CH_2−ONB), 1.95 (s, 3H, C(CN)CH_3). ^{13}C NMR (300 MHz, $CDCl_3$), δ (TMS, ppm): 219.5 (C(=S)S), 170.8 (C(=O)C), 161.6 (C−O, phenyl of ONB), 144.4 (C-C(=S)S), 140.8 (C−NO_2), 134.9 (C−CH_2, phenyl of ONB), 133.9 (*p*-C−C(=S)S), 128.6 (*m*-C−C(=S)S), 128.0 (*o*-C−C(=S)S), 126.6 (CN), 118.4 (*o*-C−C−NO_2, phenyl of ONB), 114.8 (*o*-C−C−O, *m*−C−C−NO_2, phenyl of ONB), 113.9(*o*-C−C−O, *o*−C−C−CH_2, phenyl of ONB), 63.6 (CC, alkyne group), 56.4 (CCH, alkyne group), 45.7 (CH_3−C−CN), 33.3 (C−C−C(−CN, −CH_3)), 29.8 (C−C−C(=O)), 24.2 (CH3).

General Procedure for RAFT Polymerizations. Styrene, CTA (1 equiv) and AIBN (0.125 equiv) were loaded into a dry Schlenk tube. The reaction mixture was degassed by three freeze−pump−thaw cycles and the flask was refilled with nitrogen. It was then stirred in a preheated oil bath at 80 °C for 15 h. For isolation of the polymer, the pink product (conversion: 20%) was precipitated three times into cold hexane and dried at 30 °C in vacuum. ^{1}H NMR (300 MHz, $CDCl_3$), δ (TMS, ppm): 8.24 (d, ONB), 7.86 (broad, SS−ArH), 7.60−7.43 (broad, SS−ArH), 7.33−7.29 (broad, ArH in PS), 5.53 (s, ONB−CH_2−O), 4.77 (s, HCC−CH_2−ONB), 2.58 (s, HCC−CH_2−ONB), 2.44−1.20 (broad, OOC−CH_2−CH_2, C(CN)CH_3, CH−CH_2 backbone in PS).

Click Reactions. PS−C≡CH (1 equiv), PEO−N_3 (2 equiv), CuBr/PMEDTA (0.3 equiv/0.3 equiv) and dioxane (2 mL per 1 g PS) were loaded into a dry Schlenk tube. The reaction mixture was degassed by three freeze−pump−thaw cycles and the flask was refilled with nitrogen. It was then stirred at room temperature for 48 h. The reaction solution was extracted 3 times by DCM/water; then all the volatiles were removed under reduced vacuum. The pink residue was washed more than 5 times by methanol (100 mL per 1 g product) and dried at 30 °C in a vacuum oven. Yield: ∼80%. ^{1}H NMR (300 MHz, $CDCl_3$), δ (TMS, ppm): 8.24 (d, 1H, ONB), 7.88 (s, CH=C in triazole), 7.85 (broad, 1H, SS−ArH), 7.60−7.43 (broad, 2H, SS−ArH), 7.33−7.29 (broad, ArH in PS), 5.50 (s, ONB−CH_2−O), 5.30 (s, trizazole−CH_2−ONB), 4.53 (broad, triazole−CH_2−CH_2−O), 3.88 (broad, triazole-CH_2−CH_2−O), 3.70−3.45 ((broad, CH_2−CH_2−O), 3.38 (s, O−CH_3), 2.44−1.20 (broad, OOC−CH_2−CH_2, C(CN)CH_3, CH−CH_2 backbone in PS).

General Procedures for Preparation of the Thin Films. The PS-*hν*-PEO BCPs were spin coated from toluene solutions onto silicon substrates and then annealed in a H_2O/THF atmosphere for 2.5 h. The film thickness was controlled by adjusting the solution concentration and the spinning speed. To cleave the PEO block, the block copolymer films were put in methanol solution under UV exposure at a wavelength of 365 nm and a dose of 5.6 J cm^{-2} (Blak-Ray Model B, UVL-56) for 12 h; then rinsed in water for 2 h.

Silica Nanodots from Nanoporous Thin Film Template. Polydimethylsiloxane (PDMS, Aldrich, M_w = 62 000 g/mol) dissolved in heptane was spin-coated onto the nanoporous films, annealed at 50 °C for 1 h to enhance the mobility of PDMS and draw the PDMS into the interstitial regions (Figure 8). Finally, the PDMS was transformed into silica by oxygen plasma treatment (1 h, 30 W, 0.2 bar O_2), simultaneous with the PS template being completely degraded.

■ ASSOCIATED CONTENT

Supporting Information. Mechanism of dimerization of the RAFT polymer and GPC traces before and after adding a reducing agent (DL-dithiothreitol, DTT), ^{1}H NMR of compound **2** and **4** in $CDCl_3$, RAFT polymerization kinetics based on CTA **5**, XPS spectra of nanoporous thin films, and TEM image of nanoporous thin film with large scale (over 2 μm × 2 μm). This material is available free of charge via the Internet at http://pubs.acs.org.

■ AUTHOR INFORMATION

Corresponding Author

*E-mail: (P.T.) theato@chemie.uni-hamburg.de; (E.B.C.) Coughlin@mail.pse.umass.edu.

■ ACKNOWLEDGMENT

Financial support from the German Science Foundation (DFG) under Grant TH 1104/4-1 and an International Collaboration in Chemistry award from the National Science Foundation (CHE 0924435) is gratefully acknowledged. This research was partly supported by the WCU (World Class University) program through the National Research Foundation of Korea funded by the Ministry of Education, Science and Technology (R31-10013). The authors thank J. Hirsch (UMass, Amherst, MA) for XPS measurement and helpful discussion.

■ REFERENCES

(1) (a) Bang, J.; Jeong, U.; Ryu, D. Y.; Russell, T. P.; Hawker, C. J. *Adv. Mater.* **2009**, *21*, 4769–4792. (b) Fasolka, M. J.; Mayes, A. M. *Annu. Rev. Mater. Res.* **2001**, *31*, 323.

(2) Leiston-Belanger, J. M.; Russell, T. P.; Drockenmuller, E.; Hawker, C. J. *Macromolecules* **2005**, *38*, 7676–7683.

(3) Lee, J. S.; Hirao, A.; Nakahama, S. *Macromolecules* **1988**, *21*, 274–276.

(4) (a) Thurn-Albrecht, T.; Steiner, R.; DeRouchey, J.; Stafford, C. M.; Huang, E.; Bal, M.; Tuominen, M.; Hawker, C. J.; Russell, T. P. *Adv. Mater.* **2000**, *12*, 787–791. (b) Bang, J.; Kim, S. H.; Drockenmuller, E.; Misner, M. J.; Russell, T. P.; Hawker, C. J. *J. Am. Chem. Soc.* **2006**, *128*, 7622–7629.

(5) (a) Coursan, M.; Desvergne, J. P.; Deffieux, A. *Macromol. Chem. Phys.* **1996**, *197*, 1599–1608. (b) Goldbach, J. T.; Russell, T. P.; Penelle, J. *Macromolecules* **2002**, *35*, 4271–4276. (c) Yurt, S.; Anyanwu, U. K.; Scheintaub, J. R.; Coughlin, E. B.; Venkataraman, D. *Macromolecules* **2006**, *39*, 1670–1672. (d) Zhang, M.; Yang, L.; Yurt, S.; Misner, M. J.; Chen, J. T.; Coughlin, E. B.; Venkataraman, D.; Russell, T. P. *Adv. Mater.* **2007**, *19*, 1571–1576.

(6) (a) Kang, M.; Moon, B. *Macromolecules* **2009**, *42*, 455–458. (b) Schumers, J. M.; Gohy, J. F.; Fustin, C. A. *Polym. Chem.* **2010**, *1*, 161–163.

(7) (a) Mayer, G.; Heckel, A. *Angew. Chew. Int. Ed.* **2006**, *45*, 4900–4921. (b) Bochet, C. G. *J. Chem. Soc. Perkins Trans.* **2002**, *2*, 125–142.

(8) (a) Eberhardt, M.; Theato, P. *Macromol. Rapid Commun.* **2005**, *26*, 1488–1493. (b) Rowe-Konopacki, M. D.; Boyes, S. G. *Macromolecules* **2007**, *40*, 879–888.

(9) "Click" chemistry has obtained great success in macromolecule science, in particular, postfunctionalization of preformed polymers through polymer reactions. See:(a) Golas, P. L.; Matyjaszewski, K. *Chem. Soc. Rev.* **2010**, *39*, 1338–1354. (b) Liu, J. Z.; Lam, J. W. Y.; Tang, B. Z. *Chem. Rev.* **2009**, *109*, 5799. (c) Qin, A.; Lam, J. W. Y.; Tang, B. Z. *Chem. Soc. Rev.* **2010**, *39*, 2522–2544. (d) Hawker, C. J.; Wooley, K. L. *Science* **2005**, *309*, 1200. (e) Helms, B.; Mynar, J. L.; Hawker, C. J.; Frechet, J. M. J. *J. Am. Chem. Soc.* **2004**, *126*, 15020–15201. (f) Quemener, D.; Davis, T. P.; Barner-Kowollik, C.; Stenzel, M. H. *Chem. Commun.* **2006**, 5051–5053. (g) Wiss, K. T.; Theato, P. *J Polym. Sci., Part A: Poly. Chem.* **2010**, *48*, 4758–4767. (h) Mansfeld, U.; Pietsch, C.; Hoogenboom, R.; Remzi Becer, R. C.; S. Schubert, U. S. *Polym. Chem.* **2010**, *1*, 1560–1598.

(10) Mao, H.; Hillmyer, M. A. *Soft Matter* **2006**, *2*, 57. (b) Mao, H.; Hillmyer, M. A. *Macromolecules* **2005**, *38*, 4038.

(11) Park, S.; Kim, B.; Xu, J.; Hofmann, T.; Ocko, B.; Russell, T. P. *Macromolecules* **2009**, *42*, 1278–1284.

(12) Thang, S. H.; Chong, Y. K.; Mayadunne, R. T. A.; Moad, G.; Rizzado, E. *Tetredron Letters* **1990**, *40*, 2435–2438.

(13) Fishman, A.; Farrah, M. E.; Zhong, J. H.; Paramanantham, S.; Carrera, C.; Lee-Ruff, E. *J. Org. Chem.* **2003**, *68*, 9843–9846.

(14) (a) , Barner-Kowollic, C. *Handbook of RAFT polymerization*: Wiley-VCH: Weinheim, Germany, 2008, (b) Willcock, H.; O'Reilly, R. K. *Polym. Chem.* **2010**, *1*, 149–157.